

Open boundary molecular dynamics

R. Delgado-Buscalioni^{1,a}, J. Sablić², and M. Praprotnik^{2,b}

¹ Departamento Física Teórica de la Materia Condensada, Universidad Autónoma de Madrid, Campus de Cantoblanco, 28049 Madrid, Spain

² Laboratory for Molecular Modeling, National Institute of Chemistry, Hajdrihova 19, 1001 Ljubljana, Slovenia

Received 17 March 2015 / Received in final form 5 May 2015

Published online 22 June 2015

Abstract. This contribution analyzes several strategies and combination of methodologies to perform molecular dynamic simulations in open systems. Here, the term *open* indicates that the *total* system has boundaries where transfer of mass, momentum and energy can take place. This formalism, which we call Open Boundary Molecular Dynamics (OBMD), can act as interface of different schemes, such as Adaptive Resolution Scheme (AdResS) and Hybrid continuum-particle dynamics to link atomistic, coarse-grained (CG) and continuum (Eulerian) fluid dynamics in the general framework of fluctuating Navier-Stokes equations. The core domain of the simulation box is solved using all-atom descriptions. The CG layer introduced using AdResS is located at the outer part of the open box to make feasible the insertion of large molecules into the system. Communications between the molecular system and the outer world are carried out in the outer layers, called buffers. These coupling preserve momentum and mass conservation laws and can thus be linked with Eulerian hydrodynamic solvers. In its simpler form, OBMD allows, however, to impose a local pressure tensor and a heat flux across the system's boundaries. For a one component molecular system, the external normal pressure and temperature determine the external chemical potential and thus the independent parameters of a grand-canonical ensemble simulation. Extended ensembles under non-equilibrium stationary states can also be simulated as well as time dependent forcings (e.g. oscillatory rheology). To illustrate the robustness of the combined OBMD-AdResS method, we present simulations of star-polymer melts at equilibrium and in sheared flow.

1 Introduction

A quite large number of molecular processes, with disparate applications, are naturally described in terms of open systems where, not only energy and momentum is exchanged with the exterior, but also mass. Molecular Dynamics (MD) simulations

^a e-mail: rafael.delgado@uam.es

^b e-mail: praprot@cmm.ki.si

are, by contrast, more easily implemented in periodic boxes, with a fixed number of particles. Theoretical approaches, based on Hamiltonian dynamics also rely on a fixed number of molecules. However, many applied situations and studies cannot be naturally described using closed systems or periodic boundaries with fixed mass per simulation volume. We could cite the solidification front of paraffins under temperature and velocity gradients, or ice formation or melting under and external heat flux (with possible heat advection due to flow), adsorption of molecules in surfaces under non-equilibrium states, or even shear rheology and extended thermodynamics of complex fluids, where the local density and pressure depends on the shear rate. A standard way to sort out these problems is to use large closed boxes in the hope that a “sound bulk phase” is established some distance away from the interesting domain (surface, nucleation site, interface, etc.); however it is not even clear that this option is correct, in particular if long distance correlations and confinement effects become relevant; and they do due to thermodynamic, hydrodynamic effects, or simple steric effects, in the case of large molecules. Another type of processes which would largely benefit having simulation of Open Boundary Molecular Dynamics (OBMD) systems are those involving mass exchange and/or chemical interaction of different species. Most of these processes have been studied in equilibrium, using Grand-Canonical Monte Carlo methods (Zeolites, reactions...). However having access to dynamic information requires solving the boundaries of the real system, and these boundaries are open. Interestingly, heat production under shear is also a problem which becomes hard once the molecules are long enough (polymers) to release enough entropy by friction. So much so that standard thermostats are not able to work properly [1] and heat extraction through boundaries seems to be the only physically correct alternative [2]. Again, this requires open boundaries which in fact, permit to generalize the boundary ensemble to different constraints [3]: isothermal, isenthalpic, isobaric, etc., allowing full, partial or zero heat removal and also different types of shear and compression (non-equilibrium) ensembles. The effect of boundary ensembles on polymeric response has been scarcely studied, despite its relevance shown in recent studies [4]. Another interesting application of open boundaries is to generalize recent efforts on multiscale simulations with MD-continuum synchronization, where a series of MD boxes are distributed over a grid and used to evaluate the momentum and heat fluxes introduced into the overlying continuum solver [5]. OBMD boxes would allow *mass transfers* (density field variations) in this promising multiscale methodology.

Indeed, sound is the fastest hydrodynamic mode so the most natural coupling between particle and continuum fluid dynamics should in principle involve mass transfer. Although incompressible formulations of hybrid models do exist and can be used for certain particular problems (water over surfaces [6]), there are still important unclear phenomena where these hybrid methods could contribute, such as nanobubbles [7], nucleation under non-equilibrium conditions (flow, heat or concentration gradients), links between mass, heat and momentum transfers in polymer rheology [5], and also as a tool to prove the concepts of extended thermodynamics in non-equilibrium complex fluids [8] or theories for non-equilibrium statistical mechanics, involving phase contraction and energy dissipation [9].

Technical difficulties and the inertia of the standard packages used by applied computational scientists, together with the “activation energy” required to implement any new methodology, are somewhat delaying the standard usage of mature hybrid methods [10]. Still, while all the problems mentioned above and many others can be tackled to some extent with different simulation methodologies, it would be certainly nice to have a unique scheme flexible enough to deal with all of them. This “ideal algorithm” would then necessarily use open boundaries, either to mimic the equilibrium (grand canonical) ensemble, to introduce heat, momentum and mass (species) at arbitrary rates or to couple an OBMD box with a continuum solver.

Imposing the boundary conditions on a particle system is the major challenge for hybrid methods. There have been two kinds of schemes presented in the literature: the state variable (Dirichlet boundary conditions) [6,11–14] and flux-exchange (Neumann boundary conditions) [10,14–16] schemes. One of the examples of the former is Schwartz alternating method [12,13,17,18], which is an iterative procedure that enables the hybrid coupling in steady states and closed systems. One of the pioneer works in this field (albeit not the first one [11]) was published by Flekkoy et al. [3], and its innovation was precisely the possibility of inserting arbitrary amounts of heat and momentum into OBMD simulation boxes, *through its boundaries* via external forces acting on the outer layers of the open box (the so called buffers). Another interesting feature of this view (the idea of external forces at the buffer) is that it can be easily adapted to impose Dirichlet boundary conditions [19] making possible to select Dirichlet or Neumann boundaries in a single OBMD scheme.

Another important pioneer work in this field, is related to coupling fine- and coarse-grained descriptions of soft matter within a particle-based framework [20]. The idea of so called Adaptive Resolution Scheme (AdResS) was to solve part of the MD simulation box using a simplified coarse-grained (CG) version of the all-atom (AA) description. More precisely, the idea was to solve the interesting part of the system with the detailed AA description, which is coupled with a CG description of the naked solvent at some distance from it. In the original AdResS, such coupling refers to mass and momentum, but not to energy. Recent generalizations of the idea permit to ensure energy transfer through the AA-CG borderland [21,22] and further works and extensions of this concept are presented in this volume, or will appear soon. Indeed, the AA is an open subsystem as it is surrounded by a CG domain, which should be much larger in size to act like a reservoir. However, AdResS formulation and all their sons and daughters methodologies, still work with closed *total* systems and cannot be adapted to arbitrary boundary conditions such as arbitrary heat, momentum or mass flow (of some species) across the system. Conceptually though it is not difficult to imagine that AdResS can be used in combination with OBMD and even connect it with a continuum solver. Such extension was proven in a couple of works for tetrahedral molecules [23] and water [24], and will be briefly summarized also in this review. Such connection opens several interesting roads because it allows the insertion of complex molecules, of arbitrary size, into the system: the CG domain acts now as an open subsystem (to the exterior) where large molecules (described by soft CG potentials) can be easily inserted using standard methods such as USHER [25,26] or variants [27]. In theory there is no limit to the size of molecules, as one could use two or more CG layers with coarser resolution. Limitations to large polymers are still alive in the long relaxation times and, if required, in how to treat entanglements at the borderland. Here, we present new results on this idea, by validation of the equilibrium state of OBMD simulations of star-polymers containing 12 arms and 73 monomers per molecule. These simulations illustrate another benefit of OBMD-AdResS simulations, which is the possibility of varying the thermodynamic state of the system (here we change its density), without the need of re-calibration of the CG (effective) potential. AdResS and OBMD are now evolving into new routes which involve combinations of well established tools, to name a few: energy exchange [21], free energy evaluation [28,29], Adaptive Resolution Monte Carlo [22], and SDPD (a Lagrangian hydrodynamic solver) as CG system; a quite natural hybridization which paradoxically have appeared just recently [30]. The numbers of papers in the field of multiscale simulation of liquids is increasing [31–53] and we refer to the reviews [14] and [19].

2 Open boundaries for MD

The present contribution intends to highlight the flexibility of OBMD simulations in terms of possible combinations with other existing “multiscale” methodologies. In what follows we briefly review a robust scheme for OBMD simulations which originally appeared in Ref. [3]. The original scheme was designed to implement heat and momentum fluxes across particle simulation boxes (Newmann boundary conditions) but it can be easily generalized to Dirichlet boundary conditions, as shown in Ref. [19].

The idea of OBMD is in fact quite simple. Consider an open MD simulation, such as that sketched in Figs. 1, 2, and 7. At this level, there are just two main parts: a core MD domain and a buffer. The core MD domain is (ideally) *sacred*, in the sense that no computational artifact is applied (at most a soft thermostat) just the good-old Newton laws acting to move the classically described atoms dynamics. Particles are free to enter or leave the core MD domain as they wander about, and enter (or leave) the Buffer. The buffer is assumed to be infinite, but this unwanted feature is changed by a condition over the mean number of particles in the buffer: which is fixed by a simple feedback algorithm (this required particle insertion and deletion, see below). The buffer is the key part of the scheme because it is the region where the exterior world “communicates” (fluxes and/or state-variables) with the MD system. In hybrid schemes the exterior world is another solver (usually a continuum fluid dynamic solver) and the communication is two-fold. The OBMD provides one the communication arrows: it is a method to *impose* fluxes (and/or state variables) across (or at) the borders of the MD system. We shall focus on flux coupling and refer to [6, 19, 54] for Dirichlet boundary conditions.

2.1 Equations of motion

Before entering into specific details on the buffer and how to evaluate the external forces there, let us write out the equations of motion of the particles in the OBMD setup. The dynamics of any particle *inside* the system (i.e. inside the MD+Buffer region) is determined by,

$$\frac{d\mathbf{r}_i}{dt} = \mathbf{v}_i \quad (1)$$

$$m_i \frac{d\mathbf{v}_i}{dt} = \mathbf{f}_i^{ad}(\{\mathbf{r}\}) + \mathbf{f}_i^{th}(\{\mathbf{v}\}) + \mathbf{f}_i^{ext}(\mathbf{r}_i) \quad (2)$$

where \mathbf{v}_i is the velocity of the particle i and m_i and \mathbf{r}_i its mass and position. The external force $\mathbf{f}_i^{ext}(\mathbf{r}_i)$ acts *only* in the buffer domains B , i.e. $\mathbf{f}_i^{ext}(\mathbf{r}_i) = 0$ if \mathbf{r}_i is not in B . We shall come back to the description of this force in Sect. 2.2. The forces \mathbf{f}_i^{ad} come from particle-particle interactions and in an standard OBMD simulation (i.e. not coupled with AdResS) they derive from the interaction potential energy $-\nabla_{\mathbf{r}_i} U(\{\mathbf{r}\})$. In Sect. 3 we discuss how to connect AdResS with OBMD and provide the corresponding expression for \mathbf{f}_i^{ad} . Finally, \mathbf{f}_i^{th} is the thermostat force which we will just briefly comment. Many OBMD applications (as those illustrated hereby) involve transfer of momentum (pressure tensor) from outside the MD domain. This requires a momentum conserving thermostat. Thus, in production runs, we use a DPD thermostat (in principle Lowe-Andersen [55] could also be used) whose force corresponds to,

$$\mathbf{f}_i^{th} = - \sum_j \gamma(r_{ij}) (\mathbf{v}_i - \mathbf{v}_j) + \tilde{\mathbf{R}}_{ij} \quad (3)$$

where $\tilde{\mathbf{R}}_{ij}$ is the fluctuating force (we refer to Ref. [56] for details of this DPD thermostat, see also [57] for a more general setup and microscopic foundation). Briefly, the

pair-wise friction matrix is of the form $\boldsymbol{\gamma} = \gamma_{\parallel} \mathbf{e}\mathbf{e} + \gamma_{\perp}(\mathbf{1} - \mathbf{e}\mathbf{e})$ so it projects friction force into the particle-particle (normal) direction $\mathbf{e}_{ij} \propto \mathbf{r}_i - \mathbf{r}_j$ and also along a perpendicular direction in the transversal plane. This transversal friction adds substantial viscosity to the system and we have kept it zero ($\gamma_{\perp} = 0$) in the present simulations. Finally the dependence on the friction kernels $\gamma_{\parallel}(r)$ with the pair-distance r was made constant (in present simulations) with a cut-off at one particle diameter, and the amplitude of the thermostat is determined by its characteristic time m/γ_{\parallel} and we have made it larger than the longest chain relaxation time τ . A “hard thermostat” (see equilibration process below) corresponds to smaller values m/γ , i.e. fast thermostating rates. To conclude with this fast presentation of the equations of motion, we note that Eqs. (1) and (2) were integrated using the Brunger, Brooks, Karplus (BBK) scheme [58].

2.2 External forces

Adding a precise (input) energy and pressure flux across the MD border requires control over the heat and work transferred. As stated, for this task OBMD uses external forces \mathbf{f}_i^{ext} acting on each particle at (each) buffer [3]. To evaluate these forces, one needs to consider the momentum and energy input created by such forces \mathbf{f}_i^{ext} over one time step Δt and equate the result to the desired amount of momentum and heat one wants to add/extract into the system. These later quantities are given by the momentum flux tensor \mathbf{J}_p and the heat flux (vector) and \mathbf{J}_e one wish to impose across each MD boundary¹. The momentum balance for a OBMD boundary of surface A is,

$$\mathbf{J}_p \cdot \mathbf{n} A \Delta t = \sum_{i \in B} \mathbf{f}_i^{ext} \Delta t + \sum_{i'} \Delta(m_{i'} \mathbf{v}_{i'}) \quad (4)$$

while the energy balance is

$$\mathbf{J}_e \cdot \mathbf{n} A \Delta t = \sum_{i \in B} \mathbf{f}_i^{ext} \cdot \mathbf{v}_i \Delta t + \sum_{i'} \Delta \epsilon_{i'}, \quad (5)$$

where index i runs over those particles which happen to be in the buffer $i \in B$ at each particular time, because as stated $\mathbf{f}_i^{ext} = 0$ outside B . \mathbf{n} is the unit vector normal to the buffer interface ($\mathbf{n} = \mathbf{x}$ in Fig. 7). The index i' runs over the particles that have entered or exited the buffer in the last time step Δt . Indeed, for the momentum change we have that $\Delta(m_{i'} \mathbf{v}_{i'}) = \pm m_{i'} \mathbf{v}_{i'}$ if the particle i' enters (+) or leaves (-). The corresponding energy change is $\Delta \epsilon_{i'} = \pm \epsilon_{i'}$. Thus, these terms of Eqs. (4) and (5) measure the momentum and energy release due to particle exchange with the exterior (incoming new particles and outgoing deleted ones). It is important to highlight that the balance of Eqs. (4) and (5) ensure that the total momentum and energy (MD system plus external domain) is conserved. Momentum conservation (either exact or on average [28]) is key to ensure, for instance, that the external pressure is transferred to the particle system *irrespective of the type of particle-particle potential acting in the buffer*. It is also important to warn the reader that in the OBMD scheme the external input of momentum and energy is introduced into the *whole* particle system; which includes the MD-region plus buffer domain. This means, in particular, that the momentum transfer across the MD-buffer interface is not instantaneously equal to the external input prescribed by that \mathbf{J}_p and \mathbf{J}_e in Eqs. (4) and (5) (for such exact instantaneous transfer one would need to correct for the flux due to internal particle

¹ The present explanation considers one single interface, but the method trivially generalizes to many (two parallel planes, a cube or some polyhedra, ...).

forces across the MD-buffer interface). As momentum is conserved, this fact does not affect steady states, however under unsteady forcing (e.g. oscillatory rheology) a certain delay might exist between the input pressure and that crossing the MD-buffer surface. Such delay is roughly the viscous time for momentum to cross the buffer and should be much smaller than the period of any applied unsteady forcing. The effect was completely negligible in unsteady simulations of water and tetrahedral molecules [23,24] although it has not been yet tested under unsteady polymer flow.

In order to properly separate momentum from heat, the force is separated in two parts:

$$\mathbf{f}_i^{ext} = \mathbf{G}(\mathbf{r}_i)\mathbf{F}^{ext} + \tilde{\mathbf{f}}_i^{ext} \quad (6)$$

where $\mathbf{F}^{ext} = \sum_{i \in B} \mathbf{f}_i^{ext}$ the total external force applied in the buffer and $\mathbf{G}(\mathbf{r}_i)$ is a weighting function ($\sum_{i \in B} \mathbf{G}(\mathbf{r}_i) = \mathbf{1}$) which in general has a tensorial form

$$\mathbf{G} = G_{\parallel} \mathbf{nn} + G_{\perp} \mathbf{tt}. \quad (7)$$

The second contribution in Eq. (6) $\tilde{\mathbf{f}}_i^{ext}$ is a fluctuating force which does not contributes to the overall momentum input in Eq. (4), i.e. $\sum_{i \in B} \tilde{\mathbf{F}}_i^{ext} = 0$. These random forces are introduced to create heat at a rate $\sum_{i \in B} \tilde{\mathbf{F}}_i^{ext} \cdot \mathbf{v}_i$. As explained in Ref. [3] the variance of the random forces can be evaluated from Eq. (5) to release/extract the desired amount of heat into/from the system in an irreversible way. On the other hand the power introduced by the total external force \mathbf{F}^{ext} provides the reversible work (rate) of the energy balance (see Ref. [3]).

Here we leave the energy transfer for another occasion and focus on momentum balance. The total force \mathbf{F}^{ext} is decomposed in its normal and tangential components,

$$\mathbf{F}^{ext} \equiv F_{\parallel}^{ext} \mathbf{n} + F_{\perp}^{ext} \mathbf{t} \quad (8)$$

where \mathbf{t} spans the perpendicular plane of the buffer interface. The way to distribute the external forces over the buffer using the weighing function $\mathbf{G}(\mathbf{r}_i)$ is not unique. First, for a given interface $\mathbf{G}(\mathbf{r}_i)$ it is chosen to depend on the particle position projected over the interface vector $\mathbf{r}_i \cdot \mathbf{n}$. Let us consider the interface $\mathbf{n} = \mathbf{x}$ so that $\mathbf{G} = \mathbf{G}(x_i)$. Second, one can select different forms of the weighting function for each direction of the applied force. From Eq. (7) this corresponds to

$$\mathbf{G}(x_i) \equiv \frac{g_{\parallel}(x_i)}{\sum_{i \in B} g_{\parallel}(x_i)} \mathbf{nn} + \frac{g_{\perp}(x_i)}{\sum_{i \in B} g_{\perp}(x_i)} \mathbf{tt}, \quad (9)$$

where the (unnormalized) weighting functions $g_{\parallel}(x)$ and $g_{\perp}(x)$ distribute normal and tangential forces according to their shape. Importantly, these weighting functions g_{\parallel} and g_{\perp} should be assigned at the beginning of the *equilibration process* (suitable choices are given in Sect. 5.3).

In summary, the force on a particle at the *buffer* (recall that $\mathbf{f}_i^{ext} = 0$ for particles outside the buffer) is,

$$\mathbf{f}_i^{ext} = G_{\parallel}(x_i)F_{\parallel}^{ext} \mathbf{n} + G_{\perp}(x_i)F_{\perp}^{ext} \mathbf{t} \quad (10)$$

with (see Eq. (4)),

$$\mathbf{F}^{ext} = A \left(\mathbf{J}_p \cdot \mathbf{n} - \frac{\sum_{i'} \Delta(m_{i'} \mathbf{v}_{i'})}{A \Delta t} \right). \quad (11)$$

2.3 Particle exchange

As stated, the buffer is also a particle reservoir. Particles are deleted once they leave the *end* of the buffer and new particles are inserted if required, as explained just below. Particle deletion and insertion is, first, a technical problem for a standard MD code working with fixed number of particles N . We have solved this problem in a relative easy way, by assigning a *zombie* label to any particle leaving the buffer towards the system's exterior. Using a conditional on this *zombie* particle label, these "dead" particles are immediately excluded from the neighbor search (we used linked cells), force loops, etc. New inserted particles are selected from the list of zombies, which then become immediately "alive" in their new position inside the system (in the buffer). Another way of "opening up" a MD code is to update N and reorder the particle list from $i = 1$ to N each time a particle leaves the system (there would be no zombies). However the *zombie* approach permits to work with a MD code with fixed N (whose value obviously has to be large enough) and it should also permit parallelization.

Once this technical problem is solved, the objective of the mass balance in the buffer is to have there a fixed average density. This is controlled by a simple algorithm,

$$\Delta N_B = (\Delta t / \tau_r) (\langle N_B \rangle - N_B), \quad (12)$$

where $\langle N_B \rangle$ and N_B are the average and the current number of particles inside a buffer, while τ_r is the characteristic relaxation time of buffer, typically of the order $\tau_r \sim O(100)$ MD time steps. A particle is deleted from the simulation whenever $\Delta N_B < 0$ or when the particle leaves the buffer-end. New particles are inserted (in the buffer) if $\Delta N_B > 0$. The insertion is carried out by an iterative algorithm called USHER, which is a Newton-Raphson-like search method on the potential energy surface [25, 26]. A new particle is inserted at potential energy E_T and its velocity can be extracted from a Maxwellian distribution at the local average velocity and temperature.

3 Adaptive resolution at the buffer

Although USHER is quite efficient, even for non-spherical molecules, like water [26], inserting polymer molecules is certain not possible using this straight forward approach. This is the point where an adaptive resolution method comes into play. The AdResS [32] permits to couple the hard AA domain with a soft CG domain, formed by much softer and simpler molecular descriptions. In this way AdResS simplifies insertions of complex molecules. The AA region (where fluid's constituent molecules are represented atomistically) is connected to the CG region (where each molecule is represented as one soft particle) through the hybrid (HY) region, where the change of degrees of freedom takes place (see Fig. 1). This change is implemented by gradually mixing the intermolecular AA and CG forces in a *momentum conserving* way. The resulting force appearing in Eq. (2), contains the contribution of all pair-wise molecule-molecule interactions,

$$\mathbf{f}_i^{ad} = \sum_{j \neq i} [w(x_i)w(x_j)\mathbf{f}_{ij}^{AA} + (1 - w(x_i)w(x_j))\mathbf{f}_{ij}^{CG}], \quad (13)$$

where \mathbf{f}_{ij}^{AA} is the all-atom (AA) force between molecules i and j and \mathbf{f}_{ij}^{CG} the soft force between CG representations of these molecules. These forces derive respectively from atomistic (AA) and coarse-grained (CG) potentials,

$$\mathbf{f}_{ij}^{AA} = -\nabla_{\mathbf{r}_{ij}} U^{AA}(\mathbf{r}_{ij}) \quad (14)$$

$$\mathbf{f}_{ij}^{CG} = -\nabla_{\mathbf{r}_{ij}} U^{CG}(\mathbf{r}_{ij}). \quad (15)$$

The “resolution” function $w(x_i)$ of some molecule i is $w = 1$ if the molecule is in the AA region and $w = 0$ if it is in CG region. In the transition domain, the value of w smoothly varies from 0 to 1. It is important to note that the resolution $w(x_i)$ applies to the center of mass of the molecule and not to the atomic degrees of freedom and intramolecular interactions. From Eq. (13) and as expected, two AA-molecules interact in a purely conservative fashion, according to their potential U^{AA} ; however for the whole (AA+HYB+CG) system Eq. (13) cannot be not derived from a potential energy. This means that energy is not strictly conserved and a thermostat should be used. Energy conserving versions of Eq. (13) (based on the potentials) have recently appeared but, by contrast, do not strictly conserve momentum and require a free energy compensation [21,28].

Another design option of the OBMD-AdResS setup is the composition of the buffer domain. Depending on the application one can choose to implement a homogeneous [23] buffer, where all the buffer is in CG level, or a heterogeneous one [24], schematically shown in Fig. 2. In this second choice, the entire particle domain is of AA resolution and there is also a part of the AA domain inside the buffer. In both cases new molecules are inserted into the region of CG resolution, which facilitates the insertion of large molecules, since molecules diffuse from CG towards AA domain and vice-versa. The homogeneous buffer can be the preferred choice in some particular cases, such as free energy evaluations, where the hybrid layer plays a central role [28,29]. However, in sheared flows or other non-equilibrium states, it requires adapting the viscosities of the CG and HY layers [23], a pre-calibration which is not required in the heterogeneous buffer [24]. New results presented hereby were obtained using an heterogeneous buffer.

4 Connection with Eulerian hydrodynamics: The triple-scale scheme

The momentum flux \mathbf{J}_p and the energy flux \mathbf{J}_e can be chosen *ad hoc* to set non-equilibrium OBMD simulations, but these quantities allow in fact to interface the OBMD simulation with higher level descriptions. Maybe for historical reasons, most of the projects to carry out such coupling, sometimes called hybrid MD, or particle-continuum scheme, involved Eulerian hydrodynamics interfacing MD. The number of papers on this subject is not small anymore and keeps growing (see [14,19] for some reviews). Finite differences were the preferred method for some authors [6], while finite volume for others [16,59]. In fact, finite volume formulations are more naturally suited for such coupling, particularly if one deals with flux coupling, which involve microscopic fluxes averaged over *volume* fluid cells. In such case the values of \mathbf{J}_p and \mathbf{J}_e imposed at the buffer should be those at the hybrid (particle-continuum) interface and depend, via interpolation, on the local values of the continuum solver. The coupling is so natural that the finite volume solver, which might include fluctuations and sound modes [10] does not need to be adapted to the hybrid scheme in any means: the fluid cells within the MD domain furnish the local values of any required quantity \mathbf{J}_p and \mathbf{J}_e (and also the local velocity, needed to impose continuity [60]). In fact, in the fluctuating hydrodynamics setup, one does not even need to average in time and instantaneous values of the microscopic \mathbf{J}_p and \mathbf{J}_e in the MD border domains, are just used in the standard Eulerian solver protocol. Dirichlet boundaries can be also imposed in similar ways.

When using the hybrid MD scheme in connection with AdResS, three methods are combined which classifies for the catching term “triple scale” scheme. Although the

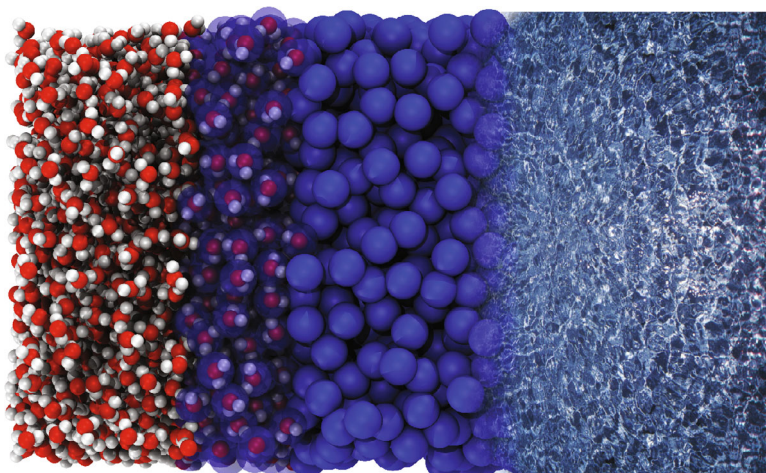


Fig. 1. An artistic illustration of the triple-scale scheme which concurrently couples the dynamics of MD (water), CG model (blue spheres) and continuum hydrodynamics [24].

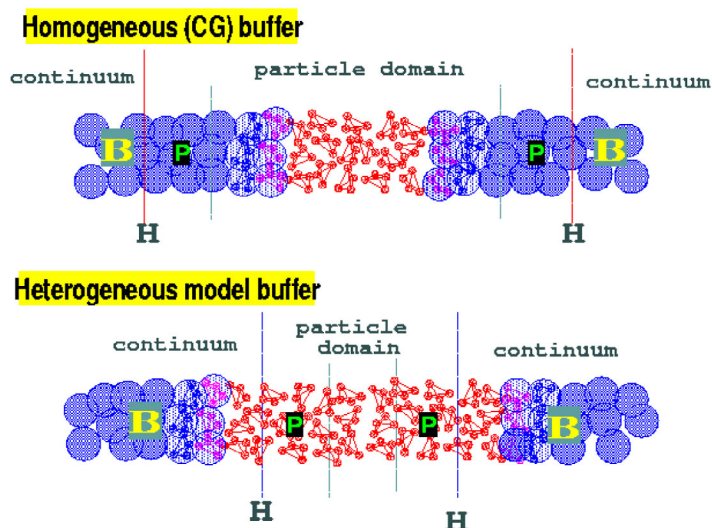


Fig. 2. Buffer: two possible setups [23].

idea of this triple scale scheme, with AdResS playing the role of the inserting facility, was meant to deal with complex molecules, so far it has been only applied on simple liquids with small molecules: tetrahedrons and water [23,24]. Equilibrium properties, i.e. radial distribution function and density profile, in MD domain of the hybrid set-up have been validated against all-atom MD simulations. And thermodynamic susceptibilities expressed in the mass fluctuations of the open MD box were shown to agree with the grand-canonical formulae [24]. These liquids were exposed to Couette and (oscillatory) Stokes flows [23,24] with excellent agreement with continuum hydrodynamics (as it should). And some technicalities were also tested: in particular using homogeneous buffer (see Fig. 2) required matching the viscosities of the CG and HY domains to that of the AA domain (softer interactions reduce viscosity). To match the CG viscosities (increasing it) it was used the transverse dissipative particle dynamics

(T-DPD) thermostat [56]. Using heterogeneous buffers [24] (see Fig. 2) avoids this step and the use of T-DPD thermostat is no longer required. The method works and awaits to deal with real applied research.

5 Simulations of star polymers

AdResS simplifies insertions of complex molecules in OBMD simulations. Although, this claim has been made in several papers, in practice, it has been so far only verified with small molecules: tetrahedrons [23] and water [24]. In this section we present new results for OBMD-AdResS simulations of much larger molecules: star polymer melts. The model of star polymers is taken from Ref. [57]. Each polymer contains 73 monomers, having 12 arms of 6 monomers attached to a central monomer. Interactions between adjacent monomers are modeled as harmonic springs and excluded volume interactions are modeled by a repulsive Weeks-Chandler-Anderson (WCA) potential. For further details on the model parameters we refer to Ref. [57], in particular the results are given in units of σ_0 , where the diameter of the monomer $\sigma = 2.415\sigma_0$, and the energy of the WCA repulsive interaction ϵ . Simulation time step equals $\Delta t = 0.01\tau$, where $\tau = \sqrt{\sigma_0^2 m_m / \epsilon}$. Here m_m represents mass of each monomer. The CG description of the polymers consists on a unique interaction site (its center of mass), so that each polymer is represented as one large CG soft ball. The CG interaction potential acting between each two CG polymers was calculated by Boltzmann iteration [61,62] so as to reproduce the radial distribution function of the center of mass of the AA description at *one* thermodynamic state: temperature $T = 4.0\epsilon/k_B$ and polymer volume fraction $\phi = 0.2$. This effective potential is shown in Fig. 3 along with the resulting radial distribution functions (RDF's) after the equilibration process of the AA polymer melt (described below). It is noted that this evaluation is carried out in a standard periodic box. Indeed the RDF's obtained in the canonical ensemble (periodic box, fixed mass) should be consistent with those obtained in the grand canonical setup (open boundaries), after the equilibration procedure. Recall however that the independent thermodynamic parameters for the open system are the external chemical potential and temperature. As stated above, for a single component $\mu = \mu(p_{ext}, T)$, so in practice μ is fixed by the input (external) normal pressure p_{ext} and temperature T . To that end, we precalculated the equation of state of the melt $p = p(T, \phi)$ in a periodic box of AA molecules and used $p_{ext} = p(4.0\epsilon/k_B, 0.2)$ as input for the open boundary simulations. Consistency obviously requires having an AA domain with polymer volume fraction $\phi = 0.2$.

We now comment on the equilibration procedure, which is usually a difficult step in polymer melt simulations [63]. We show that AdResS can be also used to alleviate this delicate process.

5.1 Equilibration procedure

To prepare the equilibrated initial configuration of star-polymer melt we use a modified version of AdResS [32], where the resolution function w is a function of time rather than of molecules' positions inside the simulation box. The resolution is, therefore, the same through out the box at any time, and is slowly sharpened from CG to AA. The force between any two molecules is given by simplified Eq. (13):

$$\mathbf{f}_{ij}^{ad} = w^2(t)\mathbf{f}_{ij}^{AA} + (1 - w^2(t))\mathbf{f}_{ij}^{CG}. \quad (16)$$

Here $w(t)$ denotes time dependent resolution function that equals 0 in CG resolution and 1 in the AA one. The corresponding expression for the force between two

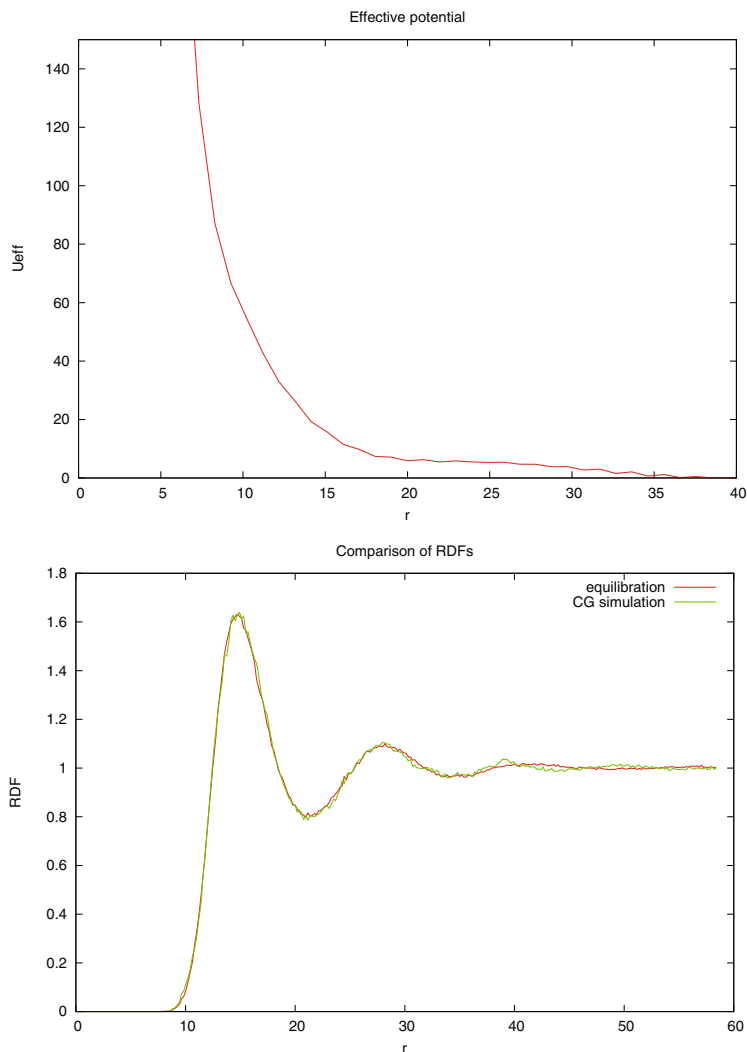


Fig. 3. Effective potential between CG particles fixed by Boltzmann Inversion at temperature $T = 4.0\epsilon/k_B$ and polymer volume fraction $\phi = 0.2$. Bottom: comparison of RDFs; the red one is obtained by equilibration procedure described in the text, and the green one by a purely CG simulation at the fixed thermodynamic state. r and U_{eff} are given in units of σ_0 and ϵ , respectively.

monomers is thus similar to the force employed in the Multigraining algorithm [64]. Note that once equilibration is finished \mathbf{f}_{ij}^{ad} equation is switched back to expression given by Eq. (13).

The equilibration is carried out in a closed system at constant temperature. First, we randomly distribute positions of CG representations of molecules inside the box. Then we simulate the system in CG resolution until it reaches the equilibrium. Afterwards, we raise the resolution function to $w = 0.01$. In order to avoid overlapping of monomers due to so far not equilibrated AA degrees of freedom, we cap the repulsive WCA potential. Then, we gradually decrease the capping radius and increase w in steps of 0.01 till the value of $w = 0.1$. Subsequently, we keep increasing w in 10 times larger steps until it reaches its AA resolution value $w = 1.0$. Finally, the equilibration

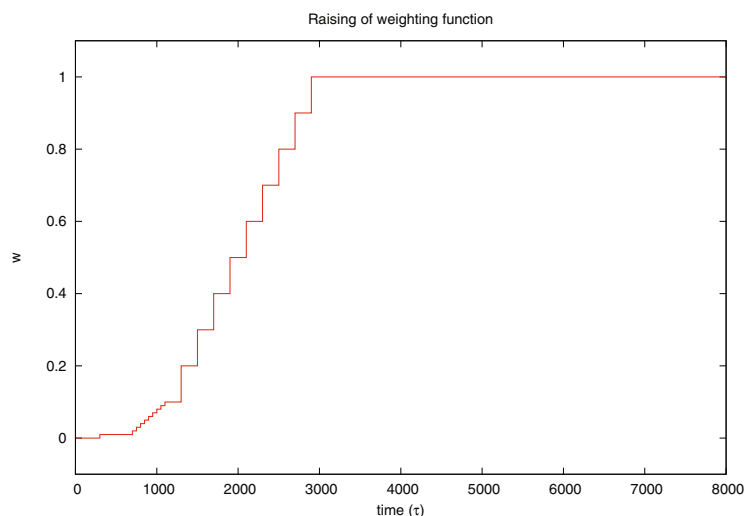


Fig. 4. The growth of w function during equilibration procedure. Equilibration in CG resolution lasts for 300τ . Then w is raised to $w = 0.01$ and for the next 100τ WCA interaction is capped at radius $r = 0.62\sigma$. In the subsequent 100τ radius of capping is decreased to $r = 0.41\sigma$ and in the last 200τ to $r = 0.21\sigma$. Afterwards, w is gradually increased in steps of 0.01 up to the value of $w = 0.1$. The equilibration is run for 50τ at each of these values. Then we keep increasing w in steps of 0.1 till its final value of $w = 1.0$, running the equilibration for 200τ at every step. Finally, the equilibration ends with 5000τ long simulation at AA resolution.

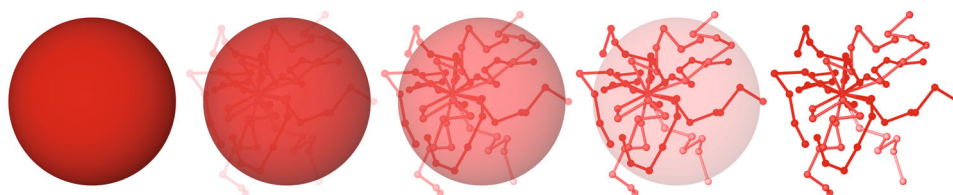


Fig. 5. Schematic representation of equilibration process. In the beginning (far left picture) each polymer is represented as a CG particle (red ball). During the equilibration process AA degrees of freedom are gradually turned on, while the CG ones are gradually turned off. At the end each polymer is modeled with the fine-grained representation (far right picture).

procedure ends with a long simulation at AA resolution. Raising of w is depicted in Fig. 4. Figure 5 demonstrates sharpening of the resolution and gradual turning on of AA degrees of freedom.

Unlike some other equilibration methods used to equilibrate melts of long polymer chains [65,66], our enables swifter disentanglement of the arms of adjacent polymers by the gradual sharpening of the resolution. At low values of w monomers feel the AA forces between them, but since the expression is multiplied by the value of w its contribution to the total force between the monomers is relatively small. Consequently, the effective radius of the monomers is smaller and this facilitates the transition of the arms. A full-blown fine-grained equilibration carried out by MD simulation would require more time as the arm disentanglement would occur more slowly.

Once the equilibration process is finished, we calculate radial distribution function (RDF) and velocity autocorrelation function of centers of mass of molecules in our melt. We compare the former with the RDF obtained from purely CG simulation

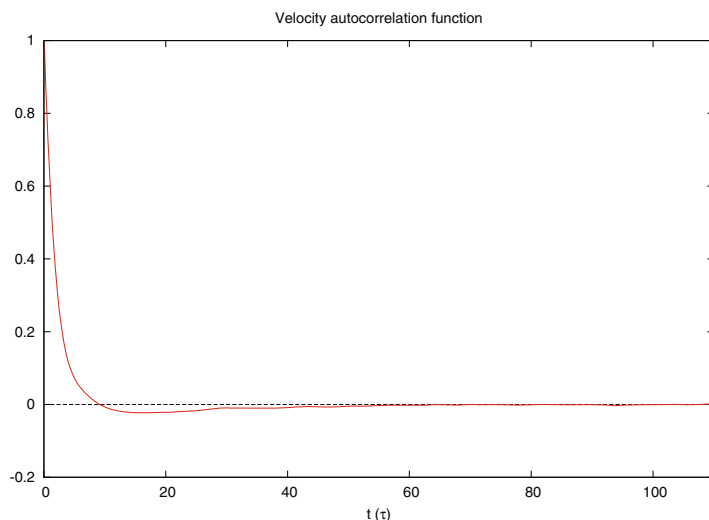


Fig. 6. Velocity autocorrelation function of the equilibrated melt.

of the melt. The comparison is demonstrated in Fig. 3. The velocity autocorrelation function is shown in Fig. 6. Its integral divided by 3 gives the diffusion constant of the melt in equilibrium, which equals $D = (0.072 \pm 0.001)\sigma_0^2/\tau$ [67], in good agreement with the results reported in Ref. [57].

In star polymers one can observe three types of relaxation phenomena [68]. First is elastic deformation of the overall shape of polymers, second relaxation occurs via rotational diffusion, and the third one regards disentanglement of arms of every star polymer. Each of the relaxation processes can be described by a corresponding autocorrelation function, which are given by Eqs. (17), (18), and (19), respectively:

$$C_R(t) = \frac{\langle R(t)R(0) - \langle R \rangle^2 \rangle}{\langle R^2 \rangle - \langle R \rangle^2} \quad (17)$$

$$C_{RD}(t) = \frac{\langle \mathbf{R}(t) \cdot \mathbf{R}(0) \rangle}{\langle R^2 \rangle} \quad (18)$$

$$C_e(t) = \frac{1}{f(f-1)} \sum_{\substack{i,j=1 \\ i \neq j}}^f \langle [\mathbf{R}_i(0) \cdot \mathbf{R}_j(0)] [\mathbf{R}_i(t) \cdot \mathbf{R}_j(t)] \rangle. \quad (19)$$

Here \mathbf{R} represents center-end vector, R end-center distance, t time, f number of arms of each polymer, and \mathbf{R}_i center-end vector for i -th arm. i and j are indices of different arms within the same polymer.

Each autocorrelation function decays with its characteristic time of the relaxation process [68, 69]. Our obtained relaxation times are the following: $\tau_R = (12 \pm 1)\tau$ for the elastic deformation of the overall shape of polymers, $\tau_{RD} = (136 \pm 5)\tau$ for rotational diffusion, and $\tau_E = (78 \pm 4)\tau$ for the relaxation occurring via arm disentanglement. We observe that the disentanglement of the arms occurs more rapidly than rotational diffusion and that is due to the short length of the arms, as each contains only 6 monomers.

From the comparison of the RDFs in Fig. 3, which match well, and from the fact that our equilibration lasted much longer than all three characteristic relaxation

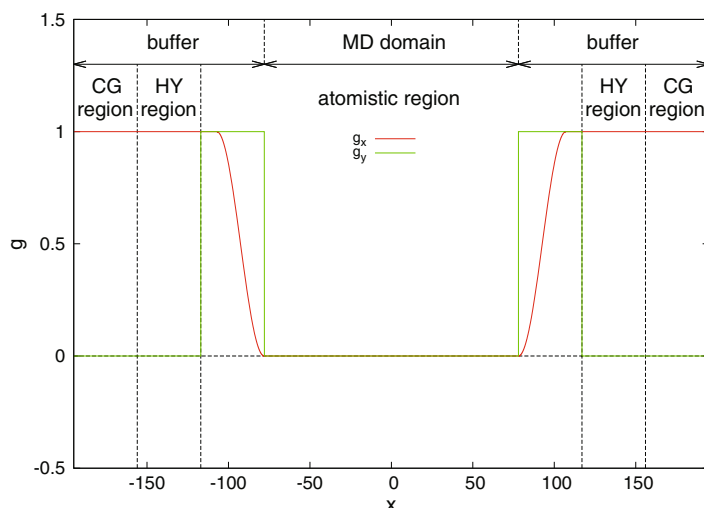


Fig. 7. Buffer distribution functions for OBMD simulations of star polymers. $g_{||}$ and g_{\perp} are the distribution functions used to impose normal pressure and shear stress to MD domain, respectively.

times we can deduce that at the end we have obtained a well equilibrated melt of star polymers.

5.2 Equilibrium OBMD simulations

After the equilibration process, we proceed with open boundary MD simulations of the star-polymer melt. An interesting check consists on modify the external pressure p_{ext} at the buffer so as to study the resulting polymer volume fraction $\phi = \phi(p_{ext})$, at fixed temperature $T = 4.0\epsilon/k_B$. The interest of this calculation resides in the possibility of using a single CG potential (which reproduces the RDF of the AA system at some thermodynamic state, here $T = 4.0\epsilon/k_B$ and $\phi = 0.2$) over a thermodynamic process where the system density changes. If the OBMD were able to recover the equation of state obtained in the canonical setup (periodic boundaries) $p = p(\phi)$, then one could use a single CG potential to simulate different thermodynamic states. This claim resembles or at least partially solves the problem of *transferability* of the CG potential [28], of central importance in mesoscopic modeling. We gradually reduced the external pressure, starting from $p_{ext} = p(0.2)$, and let the open system relax to the equilibrium density. The resulting relation between the density and external pressure was then compared with the equation of state $p = p(\phi)$ calculated in a series of canonical MD simulations (periodic boxes), where the input density was gradually reduced. Finally, we monitored the internal pressure of the AA domain in the grand canonical simulations at the different equilibrium states (varying ϕ) the system relaxes. The comparison of the three evaluations, shown in Fig. 8, shows an excellent agreement. This result is not only a way of validating the OBMD scheme, but also an indication that it is possible to simulate thermodynamic processes with large density variations using a single form of the CG potential. The reason underlying this nice feature was already explained in Ref. [24], where we showed that our approach is robust against the details of the mesoscopic model. Pressure is a flux of momentum so it just requires momentum conservation to consistently spread over the heterogeneous system. OBMD and AdResS conserves momentum so the external pressure applied

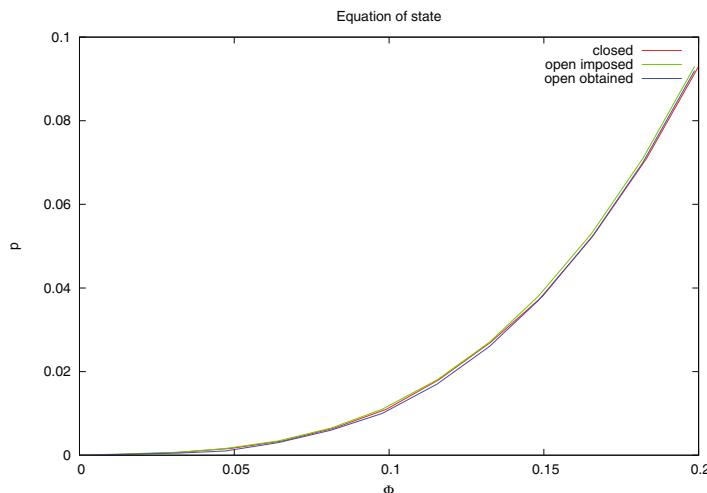


Fig. 8. Equation of state for melt of star polymers obtained by closed and OBMD simulations in equilibrium. The dependence of pressure, given in units of ϵ/σ_0^3 , on volume fraction for the melt of star polymers, each containing 12 arms of 6 monomers attached to the central monomer. Equation of state in closed systems (red) is obtained by varying system's density and calculating the pressure, to which the system relaxes. In open system, the equation of state is calculated by varying externally imposed pressure and observing the density to which the system relaxes. The imposed pressure and calculated pressure dependence on the density are depicted in green and blue, respectively. All three equations of state match well within the error bar, which is around 5%.

at the buffer is transferred without losses to the whole particle system. The same reasoning could be used for energy (temperature changes), although in this case one should use the energy conserving version of AdResS [21, 28].

5.3 Star-polymer melt under shear

To conclude with these preliminary results on open boundary MD simulations of polymer melts, we present some non-equilibrium states, focusing on steady shear. It is noted that the OBMD allows for the imposition of arbitrary time dependent external pressure tensor (either shear or compression). Here, we just show a simple shear flow to illustrate the method and how one can play with the distribution functions for normal and forces in the buffer [19] (respectively $g_{||}(x)$ and $g_{\perp}(x)$). These functions are illustrated in Fig. 7 and appear in Eq. (10). The user is free to distribute the shear stress and the normal external forces in different ways. Here, we decided to apply the normal forces over the whole buffer, while the shear stress is just distributed the AA part of the heterogeneous buffer (see Fig. 7). In fact, what we wanted to obtain is exactly the velocity profile depicted in Fig. 9 (top panel). Note that the shear rate is constant over the interesting part of the AA domain and goes to zero at the HY and CG parts of the buffer, where *no shear forces are in fact imposed*. This conservative choice ensures that viscous transport of momentum is *not* propagated outwards, towards the CG domain, and all the input stress propagates to the AA domain. To get a perfect zero shear rate at the CG domain one certainly need to provide the new inserted molecules with the local buffer velocity (as indicated in Ref. [60]). We tried other choices for g_{\perp} and found that deviations are in any case small. The case shown in Fig. 9 corresponds to a moderate shear rate (Weissenberg number

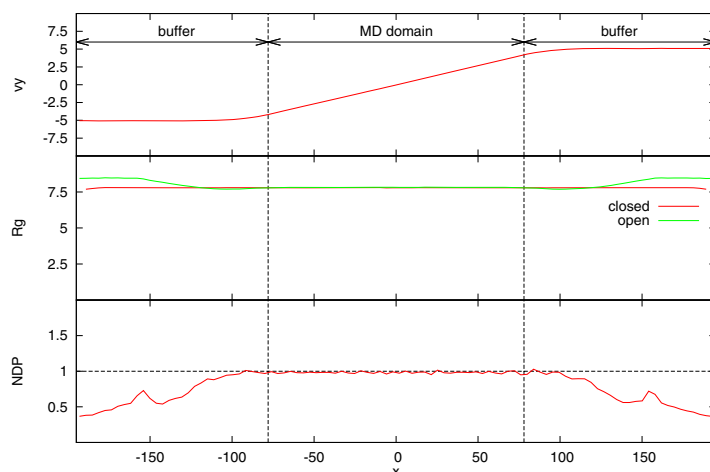


Fig. 9. Velocity (top), radius of gyration (middle), and density (bottom) profiles of star-polymer melt under shear flow. The radius of gyration profile is compared with the one obtained in a closed all-atom simulation showing a perfect agreement. The number density of particles (NDP) (normalized with the equilibrium value, which corresponds to a polymer volume fraction of $\phi = 0.2$) is also consistent with the equilibrium equation of state. Simulations corresponds to a relatively small Weissenberg number of $Wi \simeq 3$.

$Wi \simeq 3$). The middle and bottom panels of this figure show the gyration radius and the density profiles. Both are flat at the AA domain and in good agreement with the values found in closed (periodic) boxes. Interestingly however, comparisons with periodic simulations under shear (Lee-Edwards) indicate that the behavior of open and closed polymeric systems is not equivalent at large shear rates. Such study of sheared star polymer melts in OBMD boxes will be the subject of our next work.

6 Summary and outlook

This contribution presents a revision of the methodologies allowing molecular simulations of open systems (i.e. with boundaries open to mass, momentum and energy exchanges). The revision is somewhat biased, due to the relatively large amount of works that have been published in recent years. However, the information given is enough for any newly interested to follow the trend to present dates.

OBMD allows to impose momentum and/or heat at the system's boundaries. It can be then used as an interface to connect MD with other methods: with any variant or evolution of the AdResS method [20–22, 29, 32, 70–72], and also with hybrid particle-continuum hydrodynamics: either based on synchronized schemes [5, 73] or domain decomposition [19], with fluctuations [10, 16] or without fluctuations [6], and either involving flux [3] or variable coupling [6, 18, 19]. To illustrate OBMD in a far from trivial scenario, we have presented open simulations of star polymer melts, where AdResS is used to allow relatively large molecules to freely flow inwards or outwards the simulation box according to the externally imposed thermo-mechanical state.

Following the spirit of this volume, we conclude with some critics to the methodology, giving possible feasible solutions. The first one concerns the equilibration of the open system which can be longer than in a periodic box because it involves dealing with sound waves across a finite system. During these equilibration periods we used a hard Langevin thermostat to damp out these oscillations, and then, upon equilibration, switch to a momentum conserving (DPD) thermostat. It is important to

note that the buffer dynamics are not designed to act as a non-reflecting boundaries for density waves and nonphysical wave reflections can take place under unsteady forcing (compressions) or transient (equilibration) periods. Recently, the reduction of reflection at the boundaries has been discussed, using the extended Galerkin projection method, which is similar to Mori-Zwanzig projection formalism [74]. Our problem might be also solved using the idea of non-reflecting boundaries, which have been proved to work quite well for fluctuating hydrodynamics [75–77]. In fact, non-reflecting boundary conditions can be extended to transverse (shear) modes as well, its implementation into particle systems could be a quite useful tool.

A second concern of OBMD is technical: most (probably all) molecular simulation packages deal with a fixed number of particles, while in OBMD codes one needs to delete or insert. This can be sorted out in different ways, but so far there have been few attempts to adapt hybrid schemes or even OBMD schemes to production packages. There are several reasons for this fact; one is the inertia of scientific production (which does not favor robust code implementation of mature ideas, but rather production of new methods or slight variants of them). Another one could be the relative small range of problems which so far seems to require simulations of *open* systems, in any of its variants (either as an open subsystem of a closed system [78] or as really open domain [3]). The lack of OBMD options in standard packages implies that open processes have to be solved in large *closed* simulation boxes. This dilemma requires extra effort from the model-development community which should prove that these novel techniques can tackle new *difficult and relevant* problems which cannot be *solved* by standard schemes or well established theories. We have given some examples of these problems in the introduction, and more examples are recently being published [5, 71, 79]. In general, we believe that energy related processes (nanobubbles bursts, critical phenomena, melting, heat adsorption, etc.) and those involving multiple species (possibly including some description of chemical reactions) will be good candidates to reaffirm the need for an “open simulation flag” in the most famous computational packages. New ideas and methods are now appearing which will surely pave the road for this step.

Over the years we have collaborated with many colleagues on the topics described in this article. We would especially like to thank K. Kremer, L. Delle Site, and J.J. Freire for useful discussions. J. S. and M. P. acknowledge financial support through grants P1-0002 and J1-4134 from the Slovenian Research Agency. R.D-B acknowledges support from Spanish MINECO projects FIS2010-22047-C05 and FIS2013-47350-C5-1-R.

References

1. R. Khare, J.J. de Pablo, A. Yethiraj, *Macromolecules* **29**, 7910 (1996)
2. S. Bernardi, B.D. Todd, D.J. Searles, *J. Chem. Phys.* **132**, 244706 (2010)
3. E.G. Flekkoy, R. Delgado-Buscalioni, P.V. Coveney, *Phys. Rev. E* **72**, 026703 (2005)
4. M. Tschopp, J.L. Bouvard, D. Ward, D. Bammann, M.F. Horstemeyer, [arXiv:1310.0728] (2013)
5. S. Yasuda, R. Yamamoto, *Phys. Rev. X* **4**, 041011 (2014)
6. X. Nie, M.O. Robbins, S. Chen, *Phys. Rev. Lett.* **96**, 134501 (2006)
7. X. Zhang, D. Lohse, *Biomicrofluidics* **4**, 041301 (2014)
8. P. Daivis, *J. Non-Newtonian Fluid Mech.* **152**, 120 (2008)
9. T. Harada, S. Sasa, *Phys. Rev. Lett.* **95**, 130602 (2005)
10. G.D. Fabritiis, R. Delgado-Buscalioni, P.V. Coveney, *Phys. Rev. Lett.* **97**, 134501 (2006)
11. S.T. O’Connell, P.A. Thompson, *Phys. Rev. E* **52**, R5792 (1995)
12. N.G. Hadjiconstantinou, A.T. Patera, *Int. J. Mod. Phys. C* **08**, 967 (1997)
13. T. Werder, J.H. Walther, P. Koumoutsakos, *J. Comput. Phys.* **205**, 373 (2005)

14. K.M. Mohamed, A.A. Mohamad, *Microfluid Nanofluid* **8**, 283 (2010)
15. E.G. Flekkoy, G. Wagner, J. Feder, *Europhys. Lett.* **52**, 271 (2000)
16. R. Delgado-Buscalioni, G. De Fabritiis, *Phys. Rev. E* **76**, 036709 (2007)
17. P.L. Lions, On the schwarz alternating method, in *First International Symposium on Domain Decomposition Methods for Partial Differential Equations*, edited by R. Glowinski (Society for Industrial and Applied Mathematics, 1998), p. 1
18. J.H. Walther, M. Praprotnik, E.M. Kotsalis, P. Koumoutsakos, *J. Comput. Phys.* **231**, 2677 (2012)
19. R. Delgado-Buscalioni, Tools for multiscale simulation of liquids using open molecular dynamics, in *Numerical Analysis of Multiscale Computations*, edited by Y.-H. R. T. Björn Engquist, Olof Runborg (Springer, 2011)
20. M. Praprotnik, L. Delle Site, K. Kremer, *J. Chem. Phys.* **123**, 224106 (2005)
21. R. Potestio, et al., *Phys. Rev. Lett.* **110**, 108301 (2013)
22. R. Potestio, et al., *Phys. Rev. Lett.* **111**, 060601 (2013)
23. R. Delgado-Buscalioni, K. Kremer, M. Praprotnik, *J. Chem. Phys.* **128**, 114110 (2008)
24. R. Delgado-Buscalioni, K. Kremer, M. Praprotnik, *J. Chem. Phys.* **131**, 244107 (2009)
25. R. Delgado-Buscalioni, P.V. Coveney, *J. Chem. Phys.* **119**, 978 (2003)
26. G. De Fabritiis, R. Delgado-Buscalioni, P.V. Coveney, *J. Chem. Phys.* **121**, 12139 (2004)
27. M.K. Borg, D.A. Lockerby, J.M. Reese, *J. Chem. Phys.* **140** (2014)
28. P. Español, et al., *J. Chem. Phys.* **142**, 064115 (2015)
29. A. Agarwal, H. Wang, C. Schütte, L. Delle Site, *J. Chem. Phys.* **141** (2014)
30. N.D. Petsev, L.G. Leal, M.S. Shell, *J. Chem. Phys.* (2015)
31. S.C. Kamerlin, S. Vicatos, A. Dryga, A. Warshel, *Annu. Rev. Phys. Chem.* **62**, 41 (2011)
32. M. Praprotnik, L. Delle Site, K. Kremer, *Annu. Rev. Phys. Chem.* **59**, 545 (2008)
33. T. Murtola, A. Bunker, I. Vattulainen, M. Deserno, M. Karttunen, *Phys. Chem. Chem. Phys.* **11**, 1869 (2009)
34. C. Peter, K. Kremer, *Soft Matter* **5**, 4357 (2009)
35. G.S. Ayton, W.G. Noid, G.A. Voth, *Curr. Opin. Struct. Biol.* **17**, 192 (2007)
36. A. Warshel, *Annu. Rev. Biophys. Biomol. Struct.* **32**, 425 (2003)
37. M. Neri, C. Anselmi, M. Cascella, A. Maritan, P. Carloni, *Phys. Rev. Lett.* **95**, 218102 (2005)
38. A.J. Rzepiela, M. Louhivuori, C. Peter, S.J. Marrink, *Phys. Chem. Chem. Phys.* **13**, 10437 (2011)
39. S. Riniker, A.P. Eichenberger, W.F. van Gunsteren, *J. Phys. Chem. B* **116**, 8873 (2012)
40. W. Han, K. Schulten, *J. Chem. Theory Comput.* **8**, 4413 (2012)
41. P. Sokkar, S.M. Choi, Y.M. Rhee, *J. Chem. Theory Comput.* **9**, 3728 (2013)
42. T.A. Wassenaar, H.I. Inglfsson, M. Prie, S.J. Marrink, L.V. Schfer, *J. Phys. Chem. B* **117**, 3516 (2013).
43. P. Sokkar, S.M. Choi, Y.M. Rhee, *J. Chem. Theory Comput.* **9**, 3728 (2013)
44. H.C. Gonzalez, L. Darr, S. Pantano, *J. Phys. Chem. B* **117**, 14438 (2013)
45. C.F. Abrams, *J. Chem. Phys.* **123**, 234101 (2005)
46. S.O. Nielsen, P.B. Moore, B. Ensing, *Phys. Rev. Lett.* **105**, 237802 (2010)
47. A. Heyden, D.G. Truhlar, *J. Chem. Theory Comput.* **4**, 217 (2008)
48. S. Artemova, S. Redon, *Phys. Rev. Lett.* **109**, 190201 (2012)
49. W.E.B. Enquist, X.T. Li, W.Q. Ren, E. Vanden-Eijnden, *CiCP* **2**, 367 (2007)
50. D.A. Fedosov, G.E. Karniadakis, *J. Comput. Phys.* **228**, 1157 (2009)
51. W.G. Noid, *J. Chem. Phys.* **139** (2013)
52. H.I. Inglfsson, et al., *WIREs Comput. Mol. Sci.* **4**, 225 (2014)
53. M. Baaden, S.J. Marrink, *Curr. Opin. Struct. Biol.* **23**, 878 (2013)
54. X. Nie, S. Chen, M.O. Robbins, *Phys. Fluids* **16**, 3579 (2004)
55. C.P. Lowe, *EPL (Europhysics Letters)* **47**, 145 (1999)
56. C. Junghans, M. Praprotnik, K. Kremer, *Soft Matter* **4**, 156 (2008)
57. C. Hijon, P. Espanol, E. Vanden-Eijnden, R. Delgado-Buscalioni, *Faraday Discuss.* **144**, 301 (2010)
58. A. Brünger, C.L. Brooks III, M. Karplus, *Chem. Phys. Lett.* **105**, 495 (1984)

59. A. Donev, J. Bell, A. Garcia, B. Alder, *Multiscale Model. Simul.* **8**, 871 (2010)
60. R. Delgado-Buscalioni, E.G. Flekkoy, P.V. Coveney, *Europhys. Lett.* **69**, 959 (2005)
61. D. Reith, M. Pütz, F.Müller-Plathe, *J. Comput. Chem.* **24**, 1624 (2003)
62. S. Bevc, C. Junghans, M. Praprotnik, *J. Comput. Chem.* **36**, 467 (2015)
63. G. Zhang, et al., *ACS Macro Letters* **3**, 198 (2014)
64. M. Christen, W.F. van Gunsteren, *J. Chem. Phys.* **124**, 154106 (2006)
65. B. Dünweg, K. Kremer, *J. Chem. Phys.* **99**, 6983 (1993)
66. R. Auhl, R. Everaers, G.S. Grest, K.Kremer, S.J. Plimpton, *J. Chem. Phys.* **119**, 12718 (2003)
67. M. Tuckerman, *Statistical Mechanics and Molecular Simulations* (Oxford Graduate Texts, Oxford University Press, UK, 2008)
68. G.S. Grest, K. Kremer, S.T. Milner, T.A. Witten, *Macromolecules* **22**, 1904 (1989)
69. G.S. Grest, K. Kremer, T.A. Witten, *Macromolecules* **20**, 1376 (1987)
70. J. Zavadlav, et al., *J. Chem. Theory Comput.* **10**, 2591 (2014)
71. J. Zavadlav, M.N. Melo, S.J. Marrink, M. Praprotnik, *J. Chem. Phys.* **140** (2014)
72. L. Delle Site, A. Agarwal, C. Junghans, H. Wang [arXiv:1412.4540] (2014)
73. M.K. Borg, D.A. Lockery, J.M. Reese, *J. Comp. Phys.* **233**, 400 (2013)
74. X. Li, *Int. J. Numer. Meth. Eng.* **99**, 157 (2014)
75. R. Delgado-Buscalioni, A. Dejoan, *Phys. Rev. E* **78**, 046708 (2008)
76. P.J. Atzberger, P.R. Kramer, C.S. Peskin, *J. Comput. Phys.* **224**, 1255 (2007)
77. J.B. Bell, A.L. Garcia, S.A. Williams, *Phys. Rev. E* **76**, 016708 (2007)
78. H. Wang, C. Hartmann, C. Schütte, L. Delle Site, *Phys. Rev. X* **3**, 011018 (2013)
79. D. Mukherji, K. Kremer, *Macromolecules* **46**, 9158 (2013)